Clock Shift in High Field Magnetic Resonance of Atomic Hydrogen

J. Ahokas,[1] J. Järvinen,[1] G. V. Shlyapnikov,[2,3] and S. Vasiliev[1,*]

[1]*Wihuri Physical Laboratory, Department of Physics, University of Turku, 20014 Turku, Finland*
[2]*Laboratoire de Physique Théorique et Modèles Statistiques, CNRS, Université Paris Sud, 91405 Orsay, France*
[3]*Van der Waals-Zeeman Institute, University of Amsterdam, 1018 XE, The Netherlands*

We have measured electron spin resonance line shifts due to collisions in atomic hydrogen gas compressed to densities $\sim 10^{18}$ cm^{-3} in a strong magnetic field (4.6 T). The shift in a doubly polarized gas is negligible, in contrast with a mixture of two hyperfine states. This difference is explained by properly including effects of quantum statistics in atomic collisions and magnetic dipolar effects. We report on the first direct measurement of the difference between the triplet and singlet s-wave scattering lengths $a_t - a_s = 60(10)$ pm, which is in agreement with existing theories.

Collisions between atoms of a gas at low temperatures lead to a shift of spectral lines, known in the field of cold gases and atomic clocks as a clock or cold collision shift (CS). It has been studied in cryogenic hydrogen masers [1], atomic fountains [2,3], optical excitations in atomic hydrogen [4], and microwave and radio frequency transitions in alkali atom gases [5,6]. Up to now, atomic hydrogen, being the simplest atomic gas, has shown a number of unresolved discrepancies between theory and experiment on a CS in a weak magnetic field [1,7].

In this Letter, we report on the measurement of electron spin resonance (ESR) line shifts in a three-dimensional gas of atomic hydrogen compressed to high densities. Like in our recent experiment with two-dimensional atomic hydrogen [8], we find a very small CS for a doubly (electron and nuclear spin) polarized gas H↓⇂. On the other hand, the presence of another hyperfine state, which has a different projection of the nuclear spin, leads to a relatively large shift. We explain this phenomenon by including effects of quantum statistics in atomic collisions. The clock shift appears due to a difference between the mean field interaction energies in the presence and absence of the rf field. A unique feature of atomic hydrogen is a smallness of both triplet and singlet scattering (interaction) amplitudes. Therefore, the weak long-range magnetic dipolar interaction becomes important, providing a shift which depends on the geometry of the system. We present the first direct measurement of the difference between the singlet and triplet s-wave scattering lengths, which is in fair agreement with existing calculations [9,10]. Our experiments demonstrate that for H atoms with certain nuclear spin projections in a strong field the s-wave interaction vanishes, like in the case of fermions [6], and nuclear spin may be used to switch electron interactions on and off.

So far, the clock shift in a cold gas has been calculated using a transparent approach. As the rf field coherently couples the initial (i) and final (f) states of an atom and the interaction is provided by binary atomic collisions, the clock (contact) shift at density n is given by [11,12]

$$\hbar \Delta\omega = g_2(\lambda_f - \lambda_i)n, \qquad (1)$$

where $\lambda_{f,i} = 4\pi\hbar^2 a_{f,i}/m$ is the coupling parameter for the $i - i$ and $f - i$ interaction, with $a_{f,i}$ being the s-wave scattering lengths, and g_2 is the two-body local correlation for the colliding atoms [13]. If the gas contains two hyperfine states, one should take the sum over all intrastate and interstate collision contributions. This simple model can be applied to transitions between internal levels which do not involve the spin of the constituents, like in optical $1s - 2s$ transitions used to detect Bose-Einstein condensation in atomic hydrogen [4]. In magnetic resonance the transitions involve spin flips, and one should consider an appropriate symmetrization with respect to the interchange of identical particles. For fermions the Pauli exclusion principle forbids scattering with zero angular momentum, and the CS vanishes [6]. For hydrogen maser and alkali atoms in zero field, the total spin basis is used, and in most cases one may disregard the internal spin structure and utilize a simple two-level model [5]. This approach does not explain the ESR line shifts observed in our work in a strong magnetic field and is reconsidered below.

We use ESR at 128 GHz to study H gas [8]. In a strong magnetic field the resonance lines are broadened by the field inhomogeneity, and one needs relatively large gas densities to resolve small collisional shifts. However, the high density poses another difficulty: Absorption of the rf power becomes large compared with other losses in the cavity, leading to a distortion and broadening of the resonance lines [14]. We succeeded in solving these problems in a sample cell (Fig. 1), where the hydrogen gas is hydraulically compressed into a small volume (EV) located in a 0.5 mm diameter channel through the lower mirror of the Fabry-Perot resonator. The gas in the EV is weakly coupled to the resonator via an evanescent rf field, extending down by the characteristic distance equal to the channel radius. The filling factor of the sample in the cavity
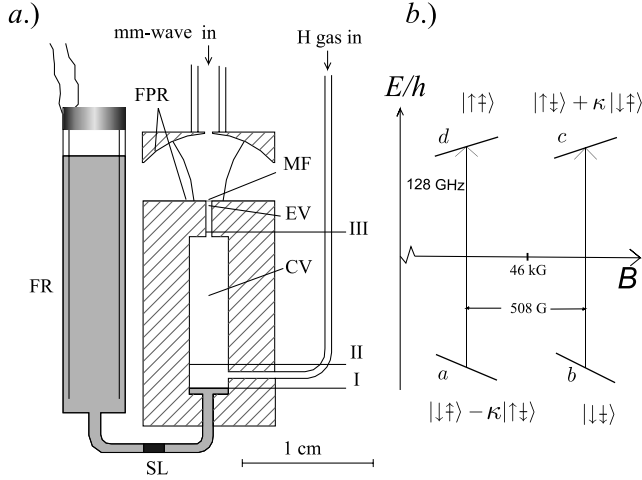
a.)

mm-wave in   H gas in

FPR

MF

EV

III

CV

FR

II

I

SL

1 cm

b.)

E/h

$|\uparrow\Uparrow\rangle$ $|\uparrow\Downarrow\rangle + \kappa|\downarrow\Downarrow\rangle$

d c

128 GHz

46 kG B

508 G

a b

$|\downarrow\Uparrow\rangle - \kappa|\uparrow\Uparrow\rangle$ $|\downarrow\Downarrow\rangle$

FIG. 1 (color online). (a) Schematic drawing of the sample cell. FPR = flat and spherical mirrors of the Fabry-Perot ESR resonator; MF = 12 μm Mylar foil; FR = fountain reservoir with liquid helium level gauge; CV = compression volume; EV = evanescent volume; SL = superleak; I, II, and III = helium level positions at different compression stages. (b) Hyperfine level diagram for a hydrogen atom in a strong magnetic field with the hyperfine mixing parameter $\kappa \approx 5.5 \times 10^{-3}$.

is reduced to $\sim 10^{-3}$, and the cavity response remains linear even at gas densities $n \approx 10^{18}$ cm^{-3}. To compress H gas, we reduce its volume by raising the helium level in the channel with the help of a fountain valve. A capacitive level gauge in the fountain reservoir (FR) allows monitoring of the helium level in the upper section of the compression volume with ~ 30 μm resolution.

We start the experiment by filling the compression volume (CV) with hydrogen atoms in hyperfine states a and b at equal densities $\approx 10^{16}$ cm^{-3} at temperatures $T = 200$–420 mK and the helium level at position I (Fig. 1). Then we raise the level to position II so that the H filling line is closed. Atoms in the mixed state a recombine much faster than those in the doubly polarized state b, and the gas rapidly evolves into the latter state, so that $p = n_b/n_a \gg 1$. The polarization ratio p depends strongly on the gas temperature and density, increasing from ~ 10 at 300 mK to $\gtrsim 100$ at $T \sim 200$ mK. A high value of p greatly improves the stability of the samples against recombination. The gas is further compressed by advancing the helium level into the EV channel (position III). By stopping the compression at different heights in the CV or EV, we can vary the compression factor up to the maximum value of ≈ 200. After completing the compression, we allow the sample to decay via recombination. The density and pressure of the sample decrease, which is detected by the decrease of the helium level in the FR and by the reduction of the ESR line integrals. The sample length decreases from 3 mm to the value determined by the He level difference in the final stage of the compression. For a sufficiently strong compression at the end of the decay, the sample evolves into a bubble, which rapidly collapses

due to the surface tension pressure of He [15]. The bubble stage is easily identified by a change in the ESR line shape. Compression to densities $\approx 10^{18}$ cm^{-3} is sensitive to the compression rate, cell temperature, and nuclear polarization. Thermal explosions [15] could be easily triggered by a too fast compression. By measuring the change of the hydrostatic head during the decays, we were able to perform an absolute density calibration of the ESR absorption integrals. Within about 10% it coincides with the calorimetrical calibration where the recombination heat is integrated during the decay.

At $n \lesssim 10^{17}$ cm^{-3}, the ESR line shape did not depend on density having the width of ≈ 70 mG caused by the inhomogeneity of the static magnetic field. At higher n, the line broadened to ≈ 250 mG and appeared to be modulated by several weak and narrow features, the position of which was changing with n and the sample height. We suggest that these features are due to spin waves, similar to magnetostatic modes in ferromagnets [16], or the spin-exchange waves [17]. These effects, to be reported elsewhere, limit the accuracy of the line position measurement to ≈ 20 mG at densities $n \approx 10^{18}$ cm^{-3}.

First, we studied the $b - c$ transition at the lowermost temperatures $T \approx 200$ mK, with the highest polarization p and the a state density being well below our detection limit of 5×10^{15} cm^{-3} (Fig. 2). These conditions are close to those in our work on the 2D gas [8]. Within the resolution of our measurements, we did not resolve any density-dependent shift of the ESR line (Fig. 3).

Next, we studied how a third hyperfine state, not involved in the resonance, influences the shift of the ESR transitions. Still working under the condition $n_b \gg n_a$, we could control the density of the a state by varying the rate and the strength of the compression and the cell temperature (Fig. 2). It was not possible to detect both lines simultaneously, since ramping the magnetic field by 507 G produces strong eddy current heating and influences the stability of the magnetic field. Therefore, we performed
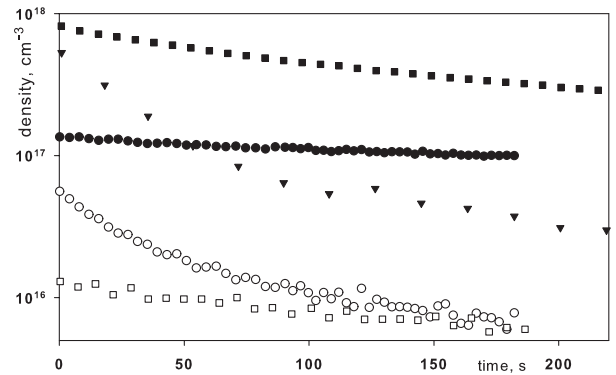

FIG. 2. Decays of the hyperfine states after different compressions. n_b (●) and n_a (○) in a low polarization sample after fast, moderate strength compression, $T = 420$ mK; n_b (■) and n_a (□) in a high polarization sample after slow compression, $T = 420$ mK; n_b (▼) in a high polarization sample, $T = 200$ mK.
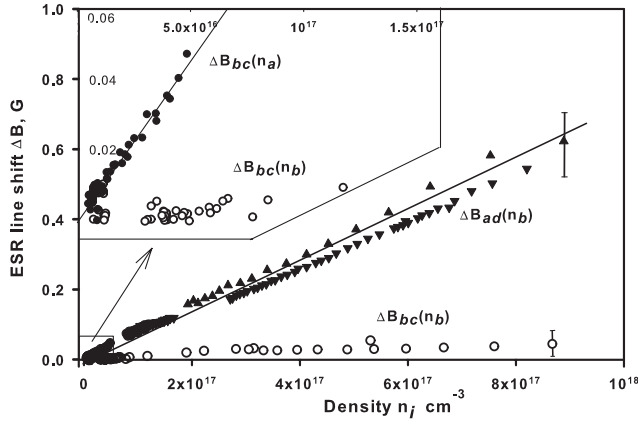
FIG. 3. Measurement of the clock shift in the mixture of hyperfine states.

two identical compressions with the same starting conditions and measured the decay of the a state for one compression and the b state decay for the other. In the mixture of hyperfine states, we get contributions from both intrastate and interstate collisions. Then the shift of the $b - c$ transition is proportional to the densities of both states: $\Delta B_{bc} = C_{bb} n_b + C_{ba} n_a$ with the coefficient C_{bb} being small, as found above. To find the contribution due to the a state, we compress the sample rapidly and examine the initial part of the decay, when n_a changes by an order of magnitude, while n_b decreases by $\sim 20\%$ only (Fig. 2). In the inset in Fig. 3, we present the data for the $b - c$ line shift as a function of n_a. We clearly see that the a state induced shift is much larger than that due to the b state. Fitting these data with both coefficients as variable parameters, we obtain $C_{bb} = 5(5) \times 10^{-20} \, \text{G cm}^3$ and $C_{ba} = 8(2) \times 10^{-19} \, \text{G cm}^3$. In a slower and stronger compression, we study the shift of the $a - d$ line. Since $n_b \gg n_a$ (Fig. 2), the shift is $\Delta B_{ad} = C_{ab} n_b + C_{aa} n_a$, with the second term being negligibly small. The data of Fig. 3 give $C_{ab} = 7(1) \times 10^{-19} \, \text{G cm}^3$, which is equal to C_{ba} within the error bars. We repeated this measurement several times (different triangles in Fig. 3) and found $\pm 20\%$ reproducibility for C_{ab}. From these experiments, we conclude that the CS is large in the presence of another hyperfine state, which is different from the initial state by the projection of the nuclear spin. Similarly to the 2D result [8], we observed a small CS, if there is only one hyperfine state present.

We now turn to the interpretation of our results. In a high magnetic field, one can omit coupling between the electron (S) and nuclear (I) spins of an atom. Accordingly, for a pair of colliding atoms S and I become good quantum numbers. We denote the electron (nuclear) singlet and triplet states as $|e_s, n_s\rangle$, $|e_s, n_t\rangle$, $|e_t, n_s\rangle$, and $|e_t, n_t\rangle$. In the Born-Oppenheimer approximation, the wave function of the colliding pair is $\Psi = \Psi_{\text{el}}(\mathbf{r}_1, \mathbf{r}_2, \mathbf{R}) \xi_S \chi_I \Phi(\mathbf{R})$, where ξ_S and χ_I are the wave functions of electron and nuclear spins, respectively, $\Psi_{\text{el}}(\mathbf{r}_1, \mathbf{r}_2, \mathbf{R})$ is the antisymmetric coordinate

wave function of electrons, and $\Phi(\mathbf{R})$ is the wave function of the relative motion of nuclei, with $\mathbf{r}_{1,2}$ and $\mathbf{R}$ being the electron coordinates and the internuclear distance, respectively. Since Ψ should be antisymmetric with respect to an interchange of electrons and nuclei (protons), for the spin configurations $|e_s, n_t\rangle$ and $|e_t, n_s\rangle$ the function $\Phi(\mathbf{R})$ is antisymmetric under interchanging the nuclei, and hence it contains only partial waves with odd orbital angular momenta l [18]. At low temperatures, the corresponding scattering amplitude is negligibly small, and these scattering channels do not contribute to the energy of interatomic interaction. For the spin configurations $|e_s, n_s\rangle$ and $|e_t, n_t\rangle$, the function $\Phi(\mathbf{R})$ is symmetric and contains partial waves with even l, in particular, the s wave ($l = 0$). At low temperatures, the s-wave scattering gives the main contribution to the interaction between atoms. For the electron singlet state $|e_s, n_s\rangle$ the scattering (interaction) amplitude is equal to the singlet scattering length a_s, and for the triplet state $|e_t, n_t\rangle$ it equals to the triplet scattering length a_t.

Under the action of an rf field, b state atoms with the density $n_b = n$ are transferred to a coherent superposition of two spin states. For instance, in the case of the $b - c$ transition in our experiment, these are b and c states. The corresponding spin wave function is then $\psi_{Sp} = \alpha \psi_b + \beta \psi_c$, where the (time-dependent) coefficients α and β satisfy the normalization condition $|\alpha|^2 + |\beta|^2 = 1$, and the quantity $|\beta|^2 n$ can be treated as the density n_c of atoms in the c state. For two colliding atoms, both in such a superposition state, the spin wave function is $\psi_{Sp}(1)\psi_{Sp}(2) = \alpha^2 \psi_b(1)\psi_b(2) + \alpha\beta[\psi_b(1)\psi_c(2) + \psi_b(2)\psi_c(1)] + \beta^2 \psi_c(1)\psi_c(2)$. It can be rewritten as $\psi_{Sp}(1)\psi_{Sp}(2) = \alpha^2 |e_{t,-1}, n_{t,-1}\rangle + \sqrt{2}\alpha\beta |e_{t,0}, n_{t,-1}\rangle + \beta^2 |e_{t,1}, n_{t,-1}\rangle$, where the subscripts $0, \pm 1$ denote the projection of the total electron (nuclear) spin. The interaction between the b components of the superposition wave function clearly has the s-wave contribution of the electron triplet channel, as well as the interaction between the c components. The same holds for the interaction between the b and c components. Then the interaction energy per unit volume between the superposition state atoms (contact interaction) will be $E_{Sp,Sp} = g_2(|\alpha|^4 \lambda_{t,-1} + 2|\alpha|^2|\beta|^2 \lambda_{t,0} + |\beta|^4 \lambda_{t,1})\frac{n^2}{2}$, corresponding to the CS $\hbar\Delta\omega_{bc} = (E_{Sp,Sp} - E_{bb})/n_c$. In the absence of the rf field, the interaction energy is $E_{bb} = g_2 \lambda_{t,-1} \frac{n^2}{2}$. Thus, assuming $|\beta| \ll 1$, we obtain the CS $\hbar\Delta\omega_{bc} = g_2(\lambda_{t,0} - \lambda_{t,1})n$, which equals zero if we neglect the dipolar interaction. This interaction is weak and anisotropic and leads to different scattering properties of the atoms with different projection of the total spin. However, the dipolar interaction is long-range, and one cannot use the pseudopotential approach for the mean field [19]. This case is treated separately, and we find the dipolar shift $\hbar\Delta\omega_{bc} = \zeta\mu_B^2 n$, where the coefficient ζ is geometry-dependent. In our experiment ζ changes from 4π to $\approx 0.3\pi$ when the sample evolves from a long cylinder into a nearly spherical bubble [20].

This gives a (very small) upper limit $C_{bb} = 5 \times 10^{-20}$ G cm^3, in agreement with our experimental data. Another reason for the nonzero CS can be a contribution of the p-wave scattering [13]. In the 2D case, there is an additional reduction of the CS caused by a ripplon-mediated interaction between H atoms [21].

The situation is drastically changed by the presence of a state atoms. In this case the interaction energy of an atom in the $b - c$ superposition state with an a state atom is $E_{Sp,a} = |\alpha|^2 E_{ba} + |\beta|^2 E_{ca}$. Then the CS is $\hbar\Delta\omega_{bc} = (E_{Sp,a} - E_{ba})/n_c$. When atoms in the states b and a approach each other, the spin configuration is $(1/\sqrt{2}) \times (|e_t, n_t\rangle + |e_t, n_s\rangle)$, and the interaction energy is $E_{ba} = \frac{1}{2}g_2\lambda_t n_b n_a$ ($g_2 = 1$ since collisions now involve distinguishable particles). For the $c - a$ interaction, the spin configuration is $\frac{1}{2}(|e_t, n_t\rangle + |e_t, n_s\rangle + |e_s, n_s\rangle + |e_s, n_t\rangle)$, and it leads to the interaction energy $E_{ca} = \frac{1}{4} \times (\lambda_t + \lambda_s)n_b n_a$. Thus we obtain $E_{Sp,a} = [\frac{|\alpha|^2}{2}\lambda_t + \frac{|\beta|^2}{4} \times (\lambda_s + \lambda_t)]n_b n_a$ for the interaction energy of the superposition state atom with an atom in the a state. Without the rf field, the interaction energy is $E_{ba} = \frac{1}{2}\lambda_t n_b n_a$. So, the clock shift is $\hbar\Delta\omega_{bc} = [\frac{\lambda_t}{2}(|\alpha|^2 - 1) + \frac{|\beta|^2}{4}(\lambda_s + \lambda_t)]/n_c$, which yields

$$\hbar\Delta\omega_{bc} = \frac{1}{4}(\lambda_s - \lambda_t)n_a = \frac{\pi\hbar^2}{m}(a_s - a_t)n. \quad (2)$$

Similarly, we obtain $\hbar\Delta\omega_{ad} = \pi\hbar^2(a_s - a_t)n_b/m$ for the shift of the $a - d$ transition due to collisions with the b state. Neglecting the weak dipolar interaction, we summarize our results in terms of intrastate shift parameters $C_{bb} = C_{aa} = 0$ and interstate ones $C_{ba} = C_{ab} = \frac{\pi\hbar}{\gamma_e m} \times (a_t - a_s)$. Note that the discussion in Ref. [22] falls into error, as it does not properly take into account local correlations of atoms.

The measurement of the interstate shift provides a direct determination of the scattering length difference $\Delta a = a_t - a_s = 60(10)$ pm. This is in the range $\Delta a = $ 40–80 pm of calculated values [10] and better matches the theories where the reduced atomic mass is used to calculate interatomic potentials (i.e., Ref. [9] gives $\Delta a = $ 48 pm). Clock shifts associated with spin-exchange effects were studied in experiments with a cryogenic hydrogen maser in weak magnetic fields [1]. However, in this case the internal energy spacing is of the same order of magnitude as the thermal energy, and one has to account for several spin-exchange channels with rates proportional to $(\Delta a)^2$. Then the shift is expressed in terms of the thermally averaged spin-exchange cross section λ_0, rather than Δa. The results of the experiments [1] significantly disagreed with the theory [7] leaving an unresolved discrepancy up to now.

In our experiments, we see that, although being composite bosons, hydrogen atoms with certain nuclear spin projections can scatter only via the p-wave (odd l-wave)

channel, and the interaction energy vanishes at low temperatures, the behavior known for fermions [6]. Therefore, in a strong field electron interactions may be switched on and off using nuclear spin of H atoms, similarly to the recent proposal to use an exchange blockade for quantum computing [23]. One can also manipulate the clock shift by varying the geometry of the system and thus changing the contribution of the magnetic dipolar interaction. The s-wave scattering length difference $a_t - a_s$ obtained in our experiments provides valuable data to judge between theories and to consider future refinements of $ab\ initio$ H-H potentials.

*servas@utu.fi

[1] M. E. Hayden and W. Hardy, Phys. Rev. Lett. **76**, 2041 (1996); M. E. Hayden, M. D. Hürlimann, and W. Hardy, Phys. Rev. A **53**, 1589 (1996).
[2] K. Gibble and S. Chu, Phys. Rev. Lett. **70**, 1771 (1993).
[3] S. Ghezali et al., Europhys. Lett. **36**, 25 (1996).
[4] D. Fried et al., Phys. Rev. Lett. **81**, 3811 (1998).
[5] D. Harber et al., Phys. Rev. A **66**, 053616 (2002).
[6] M. Zwierlein et al., Phys. Rev. Lett. **91**, 250404 (2003).
[7] S. Kokkelmans and B. Verhaar, Phys. Rev. A **56**, 4038 (1997).
[8] J. Ahokas et al., Phys. Rev. Lett. **98**, 043004 (2007).
[9] M. J. Jamieson and B. Zygelman, Phys. Rev. A **64**, 032703 (2001).
[10] S. Chakraborty et al., Eur. Phys. J. D **45**, 261 (2007), and references therein.
[11] S. Kokkelmans et al., Phys. Rev. A **56**, R4389 (1997).
[12] M. Öktel, T. Killian, D. Kleppner, and L. Levitov, Phys. Rev. A **65**, 033617 (2002).
[13] The contribution of the scattering at nonzero orbital angular momenta and the energy-dependent part of the s-wave scattering contribution, omitted in Eq. (1), in atomic **H** do not exceed 5% at temperatures below 420 mK used in our experiments (see [10]).
[14] S. A. Vasilyev et al., Appl. Magn. Reson. **3**, 1061 (1992).
[15] T. Tommila et al., Phys. Rev. B **36**, 6837 (1987).
[16] L. Walker, Phys. Rev. **105**, 390 (1957).
[17] B. R. Johnson et al., Phys. Rev. Lett. **52**, 1508 (1984).
[18] M. J. Jamieson et al., Phys. Rev. A **61**, 014701 (1999).
[19] L. Santos et al., Phys. Rev. Lett. **85**, 1791 (2000).
[20] A detailed calculation of ζ will be published elsewhere.
[21] K. Hazzard and E. Mueller, Phys. Rev. Lett. **101**, 165301 (2008).
[22] A. I. Safonov et al., JETP Lett. **87**, 23 (2008).
[23] D. Hayes, P. Julienne, and I. H. Deutch, Phys. Rev. Lett. **98**, 070501 (2007).